JOC The Journal of Organic Chemistry

Article

pubs.acs.org/joc

Cooperative Binding of Cucurbit[*n*]urils and β-Cyclodextrin to Heteroditopic Imidazolium-Based Guests

Petra Branná,[†] Jarmila Černochová,[†,‡] Michal Rouchal,[†] Petr Kulhánek,[§] Martin Babinský,[§] Radek Marek,[§,∥] Marek Nečas,[§,∥] Ivo Kuřitka,[‡] and Robert Vícha*[,†]

[†]Department of Chemistry, Faculty of Technology, Tomas Bata University in Zlín, Vavrečkova 275, 760 01 Zlín, Czech Republic

[‡]Polymer Centre, Tomas Bata University in Zlín, Vavrečkova 275, 760 01 Zlín, Czech Republic

[§]CEITEC-Central European Institute of Technology, Faculty of Science, Masaryk University, Kamenice 5, 625 00 Brno, Czech Republic

[∥]Department of Chemistry, Faculty of Science, Masaryk University, Kamenice 5, 625 00 Brno, Czech Republic

Supporting Information

ABSTRACT: Imidazolium-based guests containing two distinct binding epitopes are capable of binding β-cyclodextrin and cucurbit[6/7]uril (CB) simultaneously to form heteroternary 1:1:1 inclusion complexes. In the final configuration, the hosts occupy binding sites disfavored in the binary complexes because of the chemically induced reorganization of the intermediate 1:1 aggregate. In addition, the reported guests are capable of binding two CBs to form either 1:2 or 1:1:1 ternary assemblies despite consisting of a single cationic moiety. Whereas the adamantane site binds CB solely via hydrophobic interactions, the CB unit at the butyl site is stabilized by a combination of hydrophobic and ion−dipole interactions.

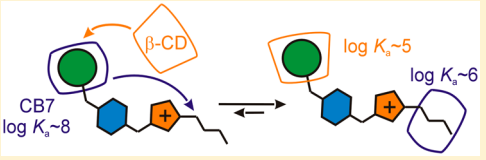

INTRODUCTION

Recently, biomimetic systems have been extensively examined because they can serve either as model systems for more complex interactions in biological chemistry or as components for constructing molecular devices. In this regard, molecules with multiple-binding epitopes play a very important role. Considering that host−guest systems are the most frequently employed approach, both hosts and guests can be designed to contain multiple-binding motifs. However, augmenting the host binding capacity is limited to either an enlargement of the single-site host interior to bind more than one guest[1] or linking two[2] or more[3] cavity motifs via appropriate covalent bridges. Although the latter approach led to impressive demonstrations of macroscopic recognition based on host−guest interactions,[4] all of the host sites in such a system are essentially independent. In addition, the only host with cooperating cavities has been reported by Isaacs and co-workers.[5] This intriguing member of the cucurbituril family, *ns*-CB10, contains two distinct interior binding sites within one large cavity and exhibits homotropic allosterism because of its ability to accommodate its cavity shape for the first bound guest. In contrast to the hosts, the guest molecules can be designed to contain an essentially unlimited number of binding sites,[6] and subsequent binding of host molecules at adjacent positions can be influenced by host−host attractive[7] or repulsive[8] interactions or guest preorganization.[9]

Among other hosts, cucurbit[*n*]urils[10] (CB*n*s) and cyclodextrins[11] (CDs) have attracted considerable attention within the scientific community. Because the macrocycles of the most prominent members of the cyclodextrin family (i.e., α-, β-, and γ-CD) consist of six, seven, and eight D-glucopyranose units, respectively, linked via α(1→4) glycosidic bonds, they are fully biocompatible and have consequently been used in several applications over the past decades in the pharmaceutical and food industries, cosmetics, and wrapping materials.[12] Because of the presence of nonpolar interior cavities and hydrophilic hydroxylated rims, CDs bind neutral guests to form water-soluble inclusion complexes with up to micromolar dissociation constants.[13] Cucurbit[*n*]urils are macrocyclic oligomers of glycoluril units doubly linked by methylene bridges. They were rediscovered for modern chemistry by Mock[14] and Kim,[15] who repeated the original procedure developed by Behrend[16] to isolate CB6 and prepare higher homologues with $n > 6$. These rigid molecules with a barrel-like hydrophobic cavity and two symmetry-equivalent rims lined with carbonyl groups are ideally structured to form inclusion complexes with nonpolar cationic guests that are held together by hydrophobic and ion−dipole interactions. In particular, dicationic guests derived from ferrocene[17] or the cage hydrocarbons adamantane,[18] diamantane,[19] and bicyclo[2.2.2]octane[18] have been reported to form ultrastable aggregates with CB7, having association constants of up to 10^{17} M^{-1}, which exceed the binding strength of the well-known avidin−biotin pair. This outstanding selectivity gave rise to the design of novel thermodynamically or kinetically driven self-sorting systems in which guests with multiple-binding epitopes play a crucial role. The pH-responsive self-sorting aggregation processes of complex mixtures consisting of CB

Received: June 29, 2016
Published: September 23, 2016

DOI: 10.1021/acs.joc.6b01564
J. Org. Chem. 2016, 81, 9595−9604

and β-CD hosts and ditopic adamantyl(alkyl)ammonium guests have been described by Issacs and co-workers.[20] The same group has reported an interesting dynamic behavior of a system comprised of CB6, CB7, and *trans*-cyclohexane-1,4-diammonium and adamantanealkyl ammonium guests. The former guest and CB6 formed an extraordinarily stable assembly with a half-life of 26 years, whereas the adamantane-based guests displayed very high affinity for CB7.[21] Subsequently, Kaifer and co-workers have described an adamantane−ferrocene ditopic guest that formed two distinct inclusion complexes with CB7 that evolved toward a thermodynamically preferred adamantane-bound adduct within 10 h.[22] In addition to the most frequently used alkylammonium and pyridinium cations, dialkylimidazolium salts have deservedly attracted the attention of supramolecular chemists because of their catalytic capacity[23] and biological activity[24] and as a source of N-heterocyclic carbene ligands.[25]

Employing multitopic guests, we describe various chemoresponsive reorganizations as hosts that competed for different binding sites. However, in the final complexes, the individual preferences of the hosts determined which binding sites were occupied. We were intrigued to examine whether small synthetic guests consisting of two different binding epitopes can overcome the individual preference of the first host by offering a second site when the initial binary complex is transformed into a heteroternary complex during the addition of the second host. Therefore, we prepared a series of new guests consisting of one adamantane-based binding site and one butyl binding site and investigated their binding behaviors in binary and ternary systems by means of NMR spectroscopy, titration calorimetry, mass spectrometry, and molecular modeling.

RESULTS AND DISCUSSION

Synthesis of Guests 1−7. The adamantylated imidazolium/benzimidazolium salts **1**−**7** (Figure 1) were prepared via the two-step procedure shown in Scheme S1. Initially, the corresponding adamantyl-bearing bromides reacted with imidazole or benzimidazole under base conditions for N1 alkylation with typical yields of 45−95%. The final quaternization was performed in neat alkyl halide or butyl mesylate. Whereas oily products had to be purified by column chromatography, solid salts were easily precipitated from the reaction mixture with diethyl ether or THF, washed with plenty of solvent, and used without further purification. The solid-state structures of $\mathbf{2}^{+}I^{-}$ and $\mathbf{2}^{+}MsO^{-}$ were determined via X-ray diffraction analysis (see the Supporting Information for further details). Because the prepared (benz)imidazolium salts were rather hygroscopic, the samples for characterization and binding studies were dried in vacuum at 50−60 °C to constant weight and stored under an inert atmosphere.

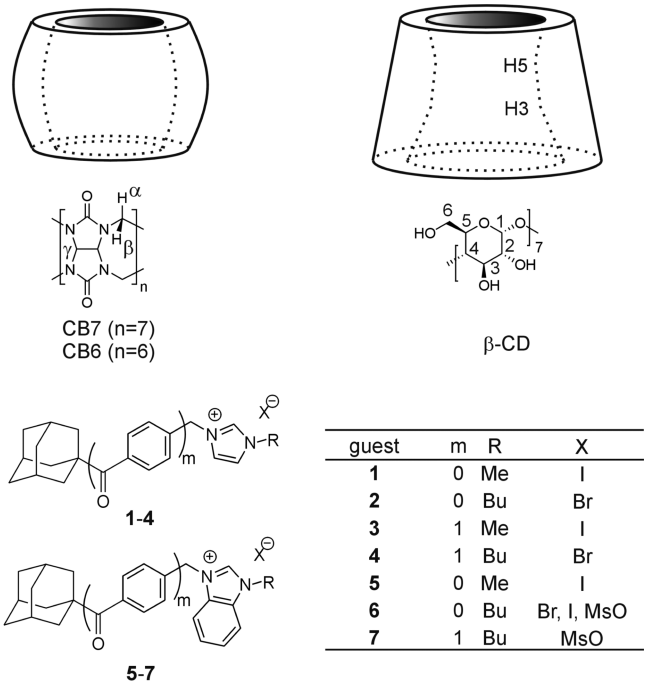

guest	m	R	X
1	0	Me	I
2	0	Bu	Br
3	1	Me	I
4	1	Bu	Br
5	0	Me	I
6	0	Bu	Br, I, MsO
7	1	Bu	MsO

Figure 1. Structures of the guests and hosts used in this work.

Binary Systems with β-CD. Initially, we investigated the binding behavior of guests **1**−**7** with CB6, CB7, and β-CD using ^{1}H NMR spectroscopy. It is well established that the guest protons inside the CB cavity are shielded (upfield shift), whereas the protons located outside the cavity, close to its portal, are deshielded (downfield shift).[1b,10a] In contrast, the interior of the β-CD cavity has, in general, only a weak deshielding effect on the atoms of the encapsulated guest, as has been demonstrated for various adamantane guests.[2a,b,d,26] Accordingly, NMR spectroscopy is very useful tool for determining the predominant binding site of the host−guest interaction. All of the examined guest/β-CD systems followed the fast-exchange regime on the NMR time scale (at defined conditions), and thus, only a single set of signals was observed for each titration. The maximal complexation-induced downfield shift of approximately 0.22 ppm for adamantane bridgehead H atoms, which was observed for all of the examined guests (**1**−**7**), unambiguously implies that β-CD binds the adamantane moiety to form an inclusion complex. The 1:1 stoichiometry of these complexes was estimated by ^{1}H NMR titrations, as shown for guests **1**, **2**, and **4** in Figure S36. Additional evidence indicating the inclusion of the adamantane moiety in the CD cavity was obtained using two-dimensional (2D) ROESY experiments. We clearly observed interactions between the H atoms of the adamantane scaffold and the inner cyclodextrin H atoms at positions 3 and 5. An example of such interactions observed in the ROESY spectrum of a 1:1 mixture of guest **2** with β-CD is given in Figure S36. The formation of 1:1 complexes was further evidenced by isothermal titration calorimetry (ITC). In addition, the values of the obtained binding constants on the order of 10^{4}−10^{5} M^{-1} (see Table 1, entries 1−8) are typical for cyclodextrin inclusion aggregates with adamantane-based guests in aqueous solutions.[13] Note that the binding strength is essentially unaffected by the replacement of imidazolium with the much more sterically hindered benzimidazolium. This β-CD binding versatility with averaged K_{imid}/K_{bimid} values of 1.05 strongly contrasts with the results obtained for CB7, which is 1000 times more selective (see below). Considering the similar cavity dimensions of CB7 and β-CD, we attribute the binding properties of β-CD to its greater flexibility, which permits ample space for both cationic structural motifs. In addition, β-CD displayed appreciably higher affinities for guests **4** and **7**, in which the methylene bridge between the adamantane cage and the heterocyclic cation was replaced with the longer carbonylbenzyl moiety.

Binary Systems with CB6 and CB7. Contrary to β-CD, CB6 and CB7 bind guests **1**−**7** in the slow-exchange regime, and two sets of ^{1}H NMR signals corresponding to free and

DOI: 10.1021/acs.joc.6b01564
J. Org. Chem. 2016, 81, 9595−9604

Table 1. Stoichiometry Parameters (n), Association Constants (K_a), and Standard Gibbs Energies ($\Delta G°$) Determined for Binary Systems by ITC Experiments at 303 K

entry	guest	host	n	K_a (M^{-1})	$-\Delta G°$ (kJ mol^{-1})
1	$\mathbf{2}^+Br^-$	β-CD[a]	1.02 ± 0.03	(4.49 ± 0.07) × 10^4	26.99 ± 0.42
2	$\mathbf{2}^+Br^-$	β-CD[b]	1.03 ± 0.02	(4.03 ± 0.05) × 10^4	26.71 ± 0.33
3	$\mathbf{4}^+Br^-$	β-CD[a]	0.98 ± 0.03	(4.60 ± 0.05) × 10^5	32.85 ± 0.36
4	$\mathbf{4}^+Br^-$	β-CD[b]	1.00 ± 0.01	(4.14 ± 0.09) × 10^5	32.58 ± 0.71
5	$\mathbf{1}^+I^-$	β-CD[a]	1.00 ± 0.03	(6.07 ± 0.06) × 10^4	27.75 ± 0.27
6	$\mathbf{6}^+Br^-$	β-CD[a]	0.99 ± 0.03	(3.80 ± 0.07) × 10^4	26.57 ± 0.49
7	$\mathbf{7}^+MsO^-$	β-CD[a]	0.95 ± 0.03	(5.38 ± 0.09) × 10^5	33.24 ± 0.56
8	$\mathbf{5}^+I^-$	β-CD[a]	1.00 ± 0.02	(5.43 ± 0.10) × 10^4	27.46 ± 0.51
9	$\mathbf{2}^+Br^-$	CB7[a,c]	1.01 ± 0.03	(4.08 ± 0.12) × 10^{11}	67.35 ± 1.98
10	$\mathbf{2}^+Br^-$	CB7[b,c]	1.02 ± 0.04	(3.14 ± 0.20) × 10^{10}	60.89 ± 3.84
11	$\mathbf{4}^+Br^-$	CB7[a]	0.73 ± 0.02, 1.34 ± 0.04	(2.27 ± 0.06) × 10^8, (8.97 ± 0.11) × 10^5	48.47 ± 1.28, 34.53 ± 0.42
12	$\mathbf{4}^+Br^-$	CB7[b]	0.64 ± 0.01, 0.70 ± 0.01	(9.03 ± 0.12) × 10^7, (3.93 ± 0.07) × 10^5	46.15 ± 0.61, 32.45 ± 0.58
13	$\mathbf{1}^+I^-$	CB7[a,c]	1.00 ± 0.01	(3.68 ± 0.21) × 10^{12}	72.89 ± 4.12
14	$\mathbf{3}^+I^-$	CB7[a,d]	1.04 ± 0.03	(2.69 ± 0.11) × 10^8	48.90 ± 2.07
15	$\mathbf{6}^+Br^-$	CB7[a,e]	1.02 ± 0.03	(7.15 ± 0.39) × 10^8	51.36 ± 2.77
16	$\mathbf{7}^+MsO^-$	CB7[a]	0.69 ± 0.03, 1.31 ± 0.02	(1.59 ± 0.03) × 10^8, (2.28 ± 0.03) × 10^5	47.57 ± 0.90, 31.08 ± 0.41
17	$\mathbf{5}^+I^-$	CB7[a,e]	0.99 ± 0.03	(2.97 ± 0.15) × 10^9	54.95 ± 2.83
18	$\mathbf{2}^+Br^-$	CB6[b]	1.05 ± 0.01	(2.99 ± 0.05) × 10^5	31.76 ± 0.53
19	$\mathbf{4}^+Br^-$	CB6[b]	0.95 ± 0.04	(1.43 ± 0.03) × 10^6	35.70 ± 0.75
20	$\mathbf{6}^+Br^-$	CB6[b]	0.97 ± 0.03	(4.18 ± 0.07) × 10^4	26.81 ± 0.45
21	$\mathbf{7}^+MsO^-$	CB6[b]	0.98 ± 0.03	(2.43 ± 0.05) × 10^5	31.24 ± 0.64

[a]Performed in water. [b]Performed in a 2.5 mM NaCl aqueous solution. [c]1,6-Hexanediamine·2HCl competitor. [d]Dopamine·HCl competitor. [e]L-Phenylalanine competitor. Titrations performed in triplicate.

complexed guests were observed. Because of the different cavity diameters,[15] CB7 can form a complex with both of the adamantyl and butyl moieties, whereas the binding of CB6 is limited to the linear butyl chain. These assumptions are consistent with our observations. The addition of CB7 to a solution of guest **1** or **5**, which possesses only an adamantane binding site, led to a significant shielding of the adamantane protons. This result indicates the formation of **1**/**5**@$CB7^{Ad}$ aggregates, as shown for **1** in Figure S38. (For the sake of clarity, the specific host position will be hereafter indicated by a superscripted "Ad" or "Bu" for the adamantyl or butyl binding site, respectively.) In contrast, we did not observe any complexation-induced NMR shift (CIS) during the titrations of guests **1** and **5** with CB6 in a 50 mM NaCl aqueous solution. The structures of guests **2** and **6** consist of two different butyl and adamantyl binding sites accessible to CB7. However, we observed shielding of only the adamantane protons (see Table S2). This suggests that CB7 predominantly binds adamantane inside its cavity with the butyl chain protruding outward toward the external environment. Because CB6 has a cavity that is narrower than that of CB7 and cannot confine the bulky adamantane, the inverse geometries for the **2**/**6**·CB6 assemblies with the butyl residue included inside the CB6 cavity were indicated by the strong shielding of the butyl protons (see Figure S39).

Subsequently, we examined the complexation of guests **1**, **2**, **5**, and **6** with CB6 and CB7 in terms of titration calorimetry to support a 1:1 stoichiometry. The ITC results are summarized in Table 1 (entries 9–21). We observed a surprisingly large number of variations in the binding strengths of imidazolium and benzimidazolium salts with CB7. In contrast, complexes formed between these guests and β-CD (see above) or CB6 display similar stabilities. For instance, the association constant for **2**@$CB7^{Ad}$ is 570 times higher than that for **6**@$CB7^{Ad}$, whereas **2**@$CB6^{Bu}$ has a K_a value that is only 7 times higher than that of **6**@$CB6^{Bu}$. (For further details, compare entries 9 and 15 and entries 18 and 20, respectively, in Table 1.) A similar disfavoring of the benzimidazolium cation was observed for **1**@$CB7^{Ad}$ and **5**@$CB7^{Ad}$ (Table 1, entries 13 and 17, respectively). Considering these observations, we attribute the differences in binding strengths to the inability of the rigid CB7 portal to accommodate the benzimidazolium cation efficiently because the bulky adamantane cage hinders guest shifting along the virtual c_7-symmetry axis of CB7. Note that distinct binding modes were reported for the imidazolium salts substituted with linear alkyl chains with different lengths, with the aromatic cationic moiety more or less buried in the CB6 cavity.[27] In contrast to this flexible binding model, it is reasonable to expect that the movement of the guest along the c_7 axis is significantly restricted with increased bulkiness.

Noteworthy results were obtained with the longer imidazolium salts **4** and **7**. In an equimolar mixture of the respective guest and CB7, strong shielding of the adamantyl protons corresponding to the complexation of the adamantane cage inside the CB7 cavity was accompanied by weak but clear shielding of the butyl protons, as depicted in Figure S40. The observed CISs are summarized in Table S2. There can be two reasonable explanations for this observation. As discussed below in more detail, one molecule of guest **4** or **7** can simultaneously bind two molecules of CB7 at the adamantane and butyl binding sites. Thus, in an equimolar mixture, two distinct 1:1 complexes (i.e., **4**@$CB7^{Ad/Bu}$ or **7**@$CB7^{Ad/Bu}$) are present in a fast equilibrium, which results in a time-averaged ^1H NMR spectrum. The second explanation is that the guest binds CB7 selectively at the adamantane site and the free portion of the long molecule is folded outside the cavity to an external shielding region. We strongly favor the latter hypothesis considering that **4**@$CB7^{Ad}$ is approximately 14 kJ mol^{-1} lower in energy than **4**@$CB7^{Bu}$ and strongly predominates in an equilibrium mixture at 30 °C (Table 1,

DOI: 10.1021/acs.joc.6b01564
J. Org. Chem. 2016, 81, 9595–9604

entry 11). In addition, very similar CISs were observed for the guest **4**/CB6 mixture. In this instance, the strong shielding of all of the butyl protons indicates that the butyl chain is inside the CB6 cavity. The small shielding of the adamantane protons can be attributed to the folding of the Ad cage back to the macrocycle exterior because the adamantane moiety is too bulky to fit inside CB6.

To further clarify this situation, we calculated the spatial distribution of isotropic magnetic shielding using a nucleus-independent chemical shielding (NICS) approach[28] around CB*n* using the methodology described in the Supporting Information. The slices through the volumetric NICS data computed for CB6 and CB7 (see Figure S86) clearly show that, apart from the expected strong shielding inside the cavity, there is also a weakly shielded region located outside the macrocycle between the carbonyl portal and the equatorial plane. Thus, any part of guest **4** located in this region will experience a weak (0.1−0.2 ppm) shielding at its atomic nuclei, which supports the hypothesis regarding back folding of guest **4** onto the exterior of CB. This bent back folding of guest **4** in complex with CB7 was further supported by molecular dynamics (MD) simulations. Figure 2 shows the superposition of snapshots

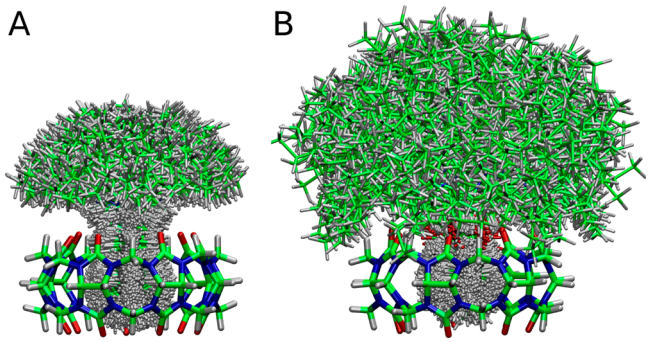

Figure 2. Overlap of guest (A) **2** and (B) **4** conformers complexed with CB7 every 1 ns from the last 900 ns of molecular dynamics simulations. Only one structure of CB7 is shown for the sake of clarity. The adamantane moiety of **2** and **4** is located inside the CB7 cavity.

from MD simulations for complexes of guests **2** and **4** with CB7. Clearly, the longer and more flexible chain of **4** can reach the external shielding region. Representative conformers of **4** and **2** superimposed with a SIMS slice for CB7 are shown in Figure S94. Additionally, the slight increase in the respective affinities of CB6 for **4** and **7** compared to those for **2** and **6** (Table 1, entries 18 and 19 and entries 20 and 21, respectively) may be attributed to the nonspecific interaction of the folded guest molecule with the CB6 exterior. However, a significant shielding of the butyl protons in the mixture of **4** and CB7 was observed as the fraction of CB7 exceeded the 1:1 ratio. The assumption that this shielding can be attributed to the formation of a 1:2 aggregate of **4**@(CB7^{Ad},CB7^{Bu}) was supported by ITC measurements in which two slopes could be clearly distinguished, indicating the presence of two distinct binding sites with respective association constants on the order of 10^8 and 10^5 M^{-1} (see Table 1, entry 11, and Figure 3). Combining the NMR and ITC results, we attributed the stronger binding event to the complexation of the adamantane site and the weaker binding event to the encapsulation of the butyl chain because the latter association constant is in good agreement with that published for 1-butyl-3-methylimidazolium with CB7.[29] The contribution of other binding modes (e.g.,

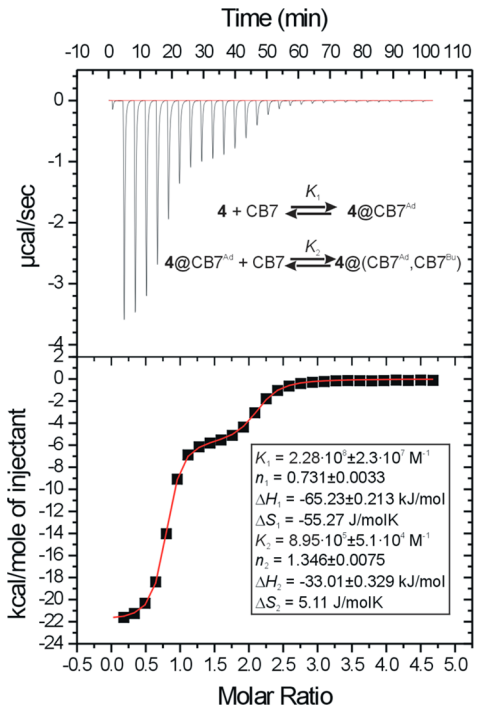

Figure 3. ITC of the complexation of 4^+Br^- with CB7 in water at 303 K. Curve fitting was performed using the two sets of sites model.

with a phenyl ring positioned inside the CB7 cavity) was excluded by using model guest **3**, which clearly displayed the formation of a 1:1 complex of **3**@CB7^{Ad} (Table 1, entry 14). In clear contrast to the **1**/**5** and **2**/**6** pairs of guests with CB7, the binding strength at the adamantane site in the **4**/**7** pair is not influenced by the chemical nature of the cation (see Table 1, entries 11 and 16). In addition, the corresponding association constants match those reported by Isaacs and co-workers for noncharged adamantane-based guests.[30] Thus, we may conclude that the ion−dipole interaction does not contribute significantly to the binding of CB7 to the adamantane site of **4**. This observation is crucial for the ability of guests **4** and **7** to simultaneously bind two cucurbituril macrocycles. To the best of our knowledge, these homoternary **4**/**7**@(CB7^{Ad},CB7^{Bu}) and heteroternary **4**/**7**@(CB7^{Ad},CB6^{Bu}) aggregates are the first well-documented complexes with two CB units compactly arranged around a single cationic moiety.

All of the discussed binary aggregates were detected using ESI-MS techniques with the exception of **6**@CB6. The ESI-MS spectra are given in Figures S71−S85.

Ternary Systems of 2 and 4 with *β*-CD, CB7, and CB6. In the next step, we examined the guest's ability to form ternary systems with two different macrocycles using representative guests **2** and **4**. To examine the binding ability of **2**, a mixture containing **2** and CB6 in a 1:1 molar ratio in 50 mM NaCl in D_2O was initially taken and examined by means of ^1H NMR titration. In this solution, the predominant arrangement is the **2**@CB6^{Bu} inclusion complex as discussed above, the formation of which is evident in Figure 4 (lines 1−3). In addition, lines 4−6 in Figure 4 show that the stepwise addition of a *β*-CD stock solution in 50 mM NaCl has a marginal effect on the positions of the butyl signals, whereas the protons of the adamantane cage experience a significant deshielding. These observations are consistent with the formation of the ternary

DOI: 10.1021/acs.joc.6b01564
J. Org. Chem. 2016, 81, 9595−9604

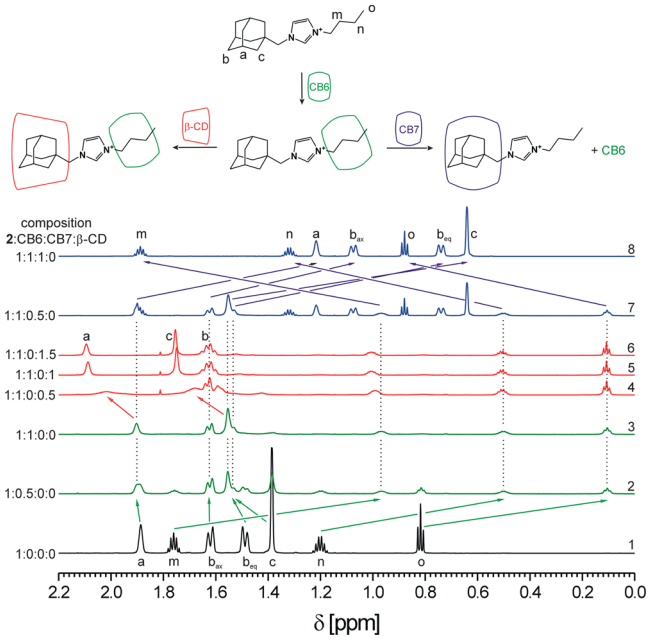

Figure 4. ^{1}H NMR spectra (700 MHz, 50 mM NaCl in D_2O, 303 K) of mixtures of **2** with CB7, β-CD, and/or CB6. The molar ratios of the mixture components are given above each line. The signal assignment is based on 2D NMR spectra.

assembly **2**@(CB6^{Bu},β-CD^{Ad}), whose geometry is schematically drawn in Figure 4.

In such a compact arrangement, the steric repulsion between the proximate CD and CB units could decrease the stability of the complex. Nevertheless, as we demonstrated using ITC, the ternary complex can be further stabilized by the formation of transient O−H···O hydrogen bonds between the OH groups of β-CD and the carbonyl oxygen atoms located on the CB portal. This additional stabilization energy, which amounts to −3.12 kJ mol^{-1}, can be calculated as the difference between the Gibbs energy obtained for the formation of **2**@β-CD^{Ad} and that for **2**@(β-CD^{Ad},CB6^{Bu}) (see Table 1, entry 1, and Table 2, entry 1). During an independent titration of a **2**@CB6^{Bu} solution with CB7, we observed a substantial shift of both the adamantane and butyl resonances. Whereas the H atoms of the adamantane cage were significantly shielded, the butyl protons were deshielded (Figure 4, lines 7 and 8). Because there is a lack of any attractive force between the two CB units due to a strong electrostatic repulsion between the two portals and as the binding strength of CB7 at the adamantane site is much higher than that for CB6 at the butyl site (K_{CB7}/K_{CB6} = 1.05 × 10^5), we may conclude that CB6^{Bu} was displaced from its initial position by CB7^{Ad}. Subsequently, we titrated an equimolar mixture of **2** and CB7 (**2**@CB7^{Ad} predominates in this solution) with β-CD. We observed significant deshielding of the imidazole H2 and H4 protons, AdC**H**$_2$, and NC**H**$_2$C**H**$_2$Et, whereas the imidazole H5 protons and N-(CH$_2$)$_2$**Et** were shielded (see Table S2). This observation can be rationalized by the formation of the ternary aggregate **2**@(CB7^{Ad},β-CD^{Bu}). The association constant for this process (K_a = 3.1 × 10^3 M^{-1}) was calculated via NMR titration (see Figure S43). We were not able to determine the association constant using ITC because of poor quality data, even after employing the highest available concentrations. In summary, guest **2** is capable of forming ternary aggregates with one CB and one β-CD unit, whereas a ternary complex consisting of two CB units was not observed.

An examination of ternary systems with guest **4** began with an equimolar solution of **4** and CB7 in which complex **4**@CB7^{Ad} predominated (shielding effect in Figure 5, lines 1−3).

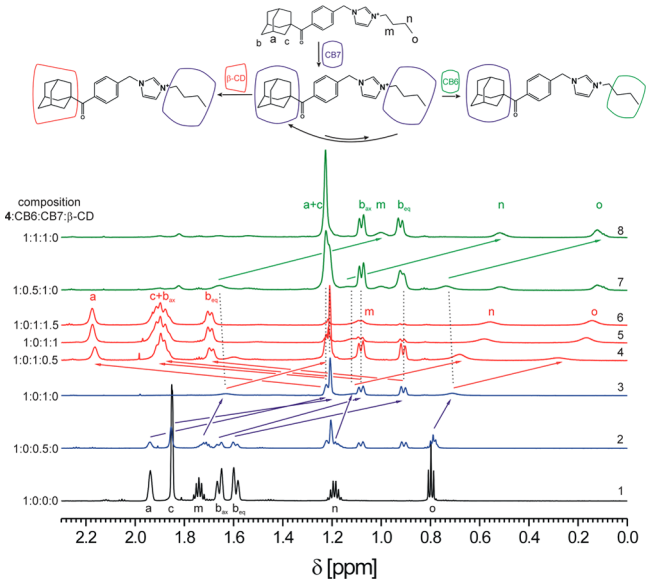

Figure 5. ^{1}H NMR spectra (700 MHz, 50 mM NaCl in D_2O, 303 K) of mixtures of guest **4** with CB7, β-CD, and/or CB6. The molar ratios of the mixture components are given above each line. The signal assignment is based on 2D NMR spectra.

Subsequent addition of CB6 led to a significant shielding of the butyl protons, whereas the positions of the adamantane NMR resonances remained essentially unaffected (Figure 5, lines 7 and 8). Total strong shielding of both the adamantane and butyl protons indicates the formation of the heteroternary complex **4**@(CB7^{Ad},CB6^{Bu}). As was discussed in the previous section, the binding of CB7 at the adamantane site is driven

Table 2. Stoichiometry Parameters (n), Experimental Association Constants (K^{exp}), and Standard Gibbs Energies ($\Delta G°$) Determined for Stepwise Complexation Reactions by ITC Experiments at 303.15 K

entry	guest	host	n	K^{exp} (M^{-1})	$-\Delta G$ (kJ mol^{-1})	$\Delta\Delta G°^a$ (kJ mol^{-1})
1	**2**@CB6	β-CD^b	0.99 ± 0.02	(1.39 ± 0.06) × 10^5	29.83 ± 0.64	−3.12 ± 0.72
2	**4**@CB6	β-CD^b	1.03 ± 0.02	(7.95 ± 0.05) × 10^5	34.23 ± 0.47	−1.65 ± 0.85
3	**4**@CB7	β-CD^c	1.04 ± 0.03	(3.10 ± 0.03) × 10^4	26.05 ± 0.50	−7.17 ± 0.87
4	**4**@CB7	CB6^b	1.03 ± 0.02	(4.66 ± 0.07) × 10^5	32.88 ± 0.64	2.82 ± 0.95

$^a\Delta\Delta G°$ values were calculated as the difference between the $\Delta G°$ of the complexed guest titration and the $\Delta G°$ of the corresponding binary titrations. ^{b}Performed in a 2.5 mM NaCl aqueous solution. ^{c}Performed in 2.5 mM NaCl in D_2O. The 1:1 **4**:CB7 ratio was verified before titration using ^{1}H NMR. Titrations were performed in triplicate.

DOI: 10.1021/acs.joc.6b01564
J. Org. Chem. 2016, 81, 9595−9604

primarily by hydrophobic interactions, leaving the butylimidazolium site free for an ion−dipole interaction with CB6. Considering the gains in energy for the formation of **4**@CB6^{Bu} and **4**@(CB7^{Ad},CB6^{Bu}) (Table 1, entry 19, and Table 2, entry 4), the free energy of such a ternary complex is approximately 3 kJ mol^{-1} higher than the value expected for a system consisting of two independent sites. This energy difference can probably be attributed to the electrostatic repulsion between the CB7 and CB6 portals. Finally, during the titration of the **4**@CB7^{Ad} complex with β-CD, we observed a significant deshielding of the adamantane protons coupled with a simultaneous NMR shielding of the butyl chain atoms (Figure 5, lines 4−6). This observation can be rationalized in the following terms. As mentioned above, CB7 can bind both the butyl and adamantyl moieties of **4**. However, in the 1:1 mixture in a 50 mM NaCl solution at 30 °C, **4**@CB7^{Ad} greatly predominates (for the corresponding ΔG, see entry 12 of Table 1). β-Cyclodextrin can also encapsulate both the adamantane cage and the butyl chain of **4** in a manner similar to that of CB7. Using titration calorimetry, we have determined the binding constant for **4** and β-CD to be 4.14×10^5 M^{-1} in a 2.5 mM NaCl aqueous solution (Table 1, entry 4). The combined ITC and NMR data clearly indicate a strong preference for a **4**@β-CD^{Ad} complex. Although it is reasonable to suppose weak binding of β-CD at the Bu site of **4**, we can exclude such a system from further discussion because the corresponding binding constant is substantially lower than that for the Ad site. Thus, both β-CD and CB7 compete for the adamantane binding site with individual binding constants of 4.14×10^5 and 9.03×10^7 M^{-1}, respectively. Notably, the NMR data indicated the expulsion of CB7 from its preferred position at the adamantane site. It is clear that the displacement of CB7 into the bulk solution is unlikely because such an event is penalized thermodynamically by ∼16 kJ mol^{-1}. However, CB7 can encapsulate the less preferred butyl chain with an approximate 35 kJ mol^{-1} gain in free energy. If this additional energy gain is considered, the overall process leading to the formation of the predominant **4**@(β-CD^{Ad},CB7^{Bu}) aggregate is thermodynamically favored with a theoretical net free energy gain of ∼19 kJ mol^{-1}. Note that the experimental value of the overall energy gain obtained from the direct titration of **4**@CB7^{Ad} with β-CD (Table 2, entry 3) is larger by approximately 7 kJ mol^{-1}. We can attribute this additional stabilization of the ternary complex to the attractive interactions between the CB7 and β-CD rims via direct or water-mediated O−H···O hydrogen bonds.

Still, a final question concerning the possible formation mechanism of **4**@(β-CD^{Ad},CB7^{Bu}) remains. In the following, we discuss the two alternative pathways that begin with the **4**@CB7^{Ad} complex as depicted in Figure 6. The first pathway involves the dissociation of **4**@CB7^{Ad} into free CB7 and guest **4** followed by the sequential binding of β-CD and CB7 at the adamantane and butyl sites, respectively. The particular order of these two binding events should be of little importance because of the very similar relative free energies of formation of **4**@CB7^{Bu} and **4**@β-CD^{Ad}. The key step of the second pathway consists of the displacement of CB7 over the guest molecule toward the nonpreferred butyl site, which is accompanied by the binding of β-CD at the adamantane site. Given the energy difference between the C and B states, the A → C pathway is strongly disfavored because the concentration of C is much lower than that of B. According to the Boltzmann distribution, the equilibrium population is more than 99.9999% of B at the expense of C considering only these two species. From a kinetic

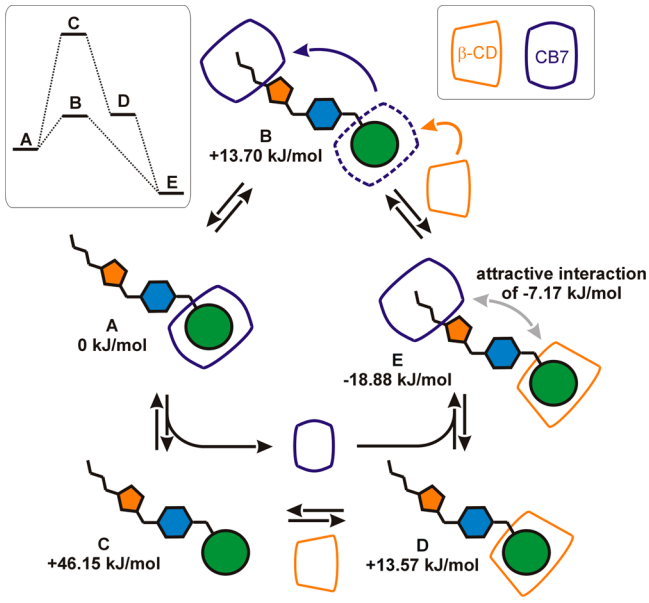

Figure 6. Possible pathways for the formation of the ternary complex **4**@(CB7^{Bu},β-CD^{Ad}). The relative free energies associated with the individual binding events were obtained from ITC experiments (2.5 mM NaCl solution, 303 K).

point of view, the most important energetic barrier is associated with the displacement of the adamantane cage through the CB7 portal. Nevertheless, both pathways result in CB7 surrendering the adamantane binding site by either leaving and entering the bulk solution or sliding toward the butyl binding site. Thus, we may conclude that the only significant difference between the A → C → D → E and A → B → E pathways lies in the energetic barrier arising from the steric hindrance associated with shuttling CB7 over the guest molecule. With regard to this, we have demonstrated previously that such movement of CB7 along guest molecules bearing similar adamantylated bisimidazolium-based structures is possible in the gas phase, even when the cationic moiety is derived from the more sterically hindered benzimidazolium core.[31]

Moreover, we have prepared separately adamantane-terminated dumbbell-like guests based on imidazolium salts bearing an additional central binding site for β-CD. When both of the terminal adamantane sites were occupied by CB7, the central site became inaccessible to β-CD.[32] This suggests that the replacement of CB7 at the adamantane site with β-CD is very unlikely. In addition, we employed MD simulations to demonstrate that the shuttling of CB7 between the adamantane and butyl sites of **4** is feasible. Initially, we positioned the CB7 unit at the butyl site and let the system develop. CB7 remained at the butyl site for 450 ns before moving to the middle phenyl site for the next 50 ns. Finally, CB7 shifted to the Ad until the end of the simulation (i.e., 500 ns). It is not surprising that only the shifting of the CB7 unit from the weaker to stronger binding site, if any, is observed within the MD simulation. However, it is reasonable to expect that the movement of CB7 is reversible. An analysis of the MD simulation can be seen in Figure S89. On this basis, we infer that the formation of **4**@(CB7^{Bu},β-CD^{Ad}) from **4**@CB7^{Ad} and β-CD can result from a chemically induced reorganization of the starting complex (i.e., A → B → E) rather than a sequence of binding and dissociation events (i.e., A → C → D/B → E). In addition to these two pathways, participation of other species that are

DOI: 10.1021/acs.joc.6b01564
J. Org. Chem. 2016, 81, 9595−9604

present in small portions in the real complex mixture should be taken into account (i.e., free **4**, **4**@CB7^{Bu}, and **4**@CB7$_2$).

Finally, the formation of the discussed ternary assemblies was confirmed in aqueous solutions using ESI-MS techniques (for comments and spectra, see the Supporting Information).

CONCLUSIONS

We synthesized four members of a new guest family (**2**, **4**, **6**, and **7**) with structures that combine the advantages of the adamantane cage and the imidazolium moiety. The supramolecular affinity for CB6, CB7, and β-CD has been investigated with the aid of additional model guests **1**, **3**, and **5**. The combination of calorimetric titrations and ^{1}H NMR spectroscopy has revealed that, in aqueous solution, both β-CD and CB7 occupy predominantly the adamantane binding sites, with association constants within the ranges of 3.8×10^4 to 5.4×10^5 M^{-1} and 1.6×10^8 to 3.7×10^{12} M^{-1}, respectively. However, CB6 was shown to bind the butyl site, with K_a values within the range of 4.2×10^4 to 1.4×10^6 M^{-1}. In strong contrast to those of CB6^{Bu} and β-CD^{Ad}, the binding strength of CB7^{Ad} was significantly reduced upon replacement of the imidazolium ring in guests **1**, **2**, **5**, and **6** (i.e., guests that contain the 1-adamantylmethyl moiety) with the benzimidazolium core. These differences can be attributed to both the inability of CB to accommodate the bulkier benzimidazolium moiety compared to β-CD and the requirement for a fixed position of the adamantane cage inside the CB7 cavity, which contrasts with the requirement for the butyl residue inside the CB6 cavity. The complete lack of CB7 selectivity toward guests **4** and **7** implies that the binding of the adamantyl group inside the CB7 cavity is driven predominantly by hydrophobic interactions, whereas the contribution of ion−dipole interactions between the imidazolium cation and the CB7 portal plays a marginal role, if any. Thus, the combination of mostly hydrophobic binding at the adamantane site with the electrostatically driven binding of the butyl chain in guests **4** and **7** allowed us to prepare compact arrangements consisting of two cucurbituril units surrounding a single imidazolium cation. Although complexes **4**/**7**@(CB7^{Ad},CB7^{Bu}) and **4**@(CB7^{Ad},CB6^{Bu}) were evidenced using ITC and NMR experiments, the calorimetric titrations demonstrated that such systems are destabilized by approximately 3 kJ mol^{-1} with respect to the individual binary complexes, most likely because of electrostatic repulsion between the CB portals. To the best of our knowledge, these results represent the first quantification of repulsion strength between two CB units, which contributes negatively to the overall stability of ternary complexes featuring these macrocycles. In addition, we were able to determine additional energetic stabilizations of -3.1 ± 0.72, -1.7 ± 0.85, and -7.2 ± 0.87 kJ mol^{-1} for complexes **2**@(β-CD^{Ad},CB6^{Bu}), **4**@(β-CD^{Ad},CB6^{Bu}), and **4**@(β-CD^{Ad},CB7^{Bu}), respectively. The overall strength of the proposed portal−portal direct or water-mediated O−H···O hydrogen bonds is comparable to that reported by Rekharsky and co-workers[7a] for CB6 and α/β-CD complexed with the dihexylammonium cation. The values of the respective stabilization energies confirm our assumptions based on the host and guest geometries. Thus, guest **2**, which possesses a distance between the binding sites that is shorter than that of guest **4**, allows for stronger interactions between β-CD and CB6. In addition, CB7, which has a portal wider than that of CB6, was shown to be more suitable for interaction with β-CD than with CB6 in ternary complexes with **4**.

The most interesting result of this work is the clear demonstration of the thermodynamically driven formation of the ternary aggregate **4**@(β-CD^{Ad},CB7^{Bu}) that features CB7 bound to an otherwise strongly disfavored butyl chain (K_{Ad}/K_{Bu} = 229.8 in a 2.5 mM NaCl aqueous solution). In addition, the formation of **4**@(β-CD^{Ad},CB7^{Bu}) from **4**@CB7^{Ad} involves a displacement of CB7^{Ad} by β-CD, which has an affinity for the adamantane site much lower than that of CB7 ($K_{CB7}/K_{\beta\text{-CD}}$ = 218.1 for the Ad site in a 2.5 mM NaCl aqueous solution). However, the energy loss related to such a displacement is compensated by the subsequent binding of CB7 to the butyl chain, which leads to an overall energetic gain of −26 kJ mol^{-1} and makes the formation of the ternary complex thermodynamically feasible. Thus, we have demonstrated that the binding behavior of multitopic guests in complex mixtures is driven by the overall energetic effect and does not always conform to the initial expectations based on knowledge of the individual binary systems. While this concept is commonly found in biological systems and complements the work of Ding et al.[33] describing self-sorting of CB8, β-CD, and the 1,6-dihydroxynaphthalene·adamantylated viologen CT complex, herein we have presented the first example of such behavior in assemblies formed by low-molecular weight synthetic guests with β-CD and CB7.

EXPERIMENTAL SECTION

General Methods. Guests **1**−**7** were prepared according to a previously published method.[32] Preparation of compounds **8** and **10** has been described previously.[31] Hosts CB6, CB7, and β-CD were purchased from commercial sources. β-CD was dried prior to use under reduced pressure at 50 °C to a constant weight. The concentrations of the CB7 solutions were determined by ITC with L-Phe as the standard. NMR spectra were recorded on a 700 MHz instrument equipped with a room-temperature (^{1}H, ^{13}C, ^{15}N) inverse triple-resonance probe. One-dimensional (1D) proton spectra were recorded at 303 K using a 7.0 kHz spectral width and a 3.3 kHz transmitter offset. Data were collected in 8−32 scans using a 1.5 s recycle delay, and 16k complex points were recorded per scan. The FIDs were apodized by a square cosine window function, zero filled to 32k complex points, and Fourier transformed to yield the resulting spectra. The 2D ROESY spectra were recorded using a spectral width of 7.0 kHz and a transmitter offset of 3.3 kHz in both dimensions and employing 150−400 ms continuous wave spinlock during the mixing period. A total of 2k complex points were collected in the t2 dimension and a total of 512 t1 increments were recorded using 16−32 scans per increment and 1.5 s recycle delay. The raw data were apodized by a squared cosine window function, zero filled to 4096 t2 and 2048 t1 points and Fourier transformed to yield the resulting 2D spectra. The residual HDO signal in both the 1D and 2D ROESY experiments was suppressed by employing presaturation during the recycle delay. No time-dependent changes in signal intensities were observed when ^{1}H NMR titration experiments were performed. The association constants and thermodynamic parameters for the complexation of guests **1**−**7** with CB7, CB6, and/or β-CD were determined by ITC. A solution of the host in water or in 2.5 mM NaCl was placed in the sample cell, to which a solution of the guest was added in a series of 20−30 injections (10 μL). The concentrations of the CB6, CB7, and β-CD solutions were determined via ITC using 1,6-hexanediamine·2HCl and 1-adamantaneamine·HCl. For the ternary systems, a solution of an equimolar mixture of the guest and host in the sample cell was titrated with a solution of the second host. The heat evolved was recorded at 303 K. The net heat effect was obtained by subtracting the heat of guest dilution from the overall observed heat effect. The association constants exceeding 10^7 M^{-1} were determined by the multistep competition method as described by Rekharsky et al.[17a] 1,6-Hexanediamine·2HCl with a K_a(H_2O) of 2.05×10^9 M^{-1} and a K_a(2.5 mM NaCl) of 2.97×10^8 M^{-1}, dopamine·HCl with a K_a(H_2O) of 4.58

DOI: 10.1021/acs.joc.6b01564
J. Org. Chem. 2016, 81, 9595−9604

$\times 10^5$ M^{-1}, and L-phenylalanine with a $K_a(H_2O)$ of 9.86×10^5 M^{-1} and a K_a(2.5 mM NaCl) of 3.01×10^5 M^{-1} were used as the competitors. The complexation enthalpies for the multistep titration experiments were calculated as a sum of enthalpies for each complexation step. The values of K obtained from competitive titrations were verified using different concentrations of competitors. The typical ITC thermograms are shown in Figure 3 and in Figures S48–S70.

*General Procedure for Preparation of **1**–**7** Bromides and Iodides.* Imidazole **8** or **9** or benzoimidazole **10** or **11** (1 equiv, see the Supporting Information for structures) was dissolved in the corresponding haloalkane (60 equiv) under an inert atmosphere. The mixture was refluxed until the starting material was consumed. After residual haloalkane had been removed under reduced pressure, the crude product was washed several times with diethyl ether. Solid products were used without further purification after being dried *in vacuo*. Oily products were purified by successive column chromatography using silica gel and 1:1 (v/v) petroleum ether/AcOEt and 1:1 (v/v) $CHCl_3$/MeOH solvents.

*General Procedure for Preparation of **6** and **7** Mesylates.* Benzoimidazole **9** or **10** (1 equiv) was dissolved in dry toluene (2 equiv), and butyl mesylate (2–3 equiv) was added at room temperature. The mixture was refluxed and monitored by TLC. When no further progress was observed, the toluene was removed *in vacuo*, and the resulting slurry was washed several times with diethyl ether. Products were purified as mentioned above.

*1-(1-Adamantylmethyl)-3-methylimidazolium Iodide (**1**$^+$**I**$^-$).* The iodide of **1**$^+$ was isolated as pale yellow crystalline powder (131 mg, 87% yield) using 90 mg (0.42 mmol) of **8**. Mp: 123–127 °C. Anal. Calcd for $C_{15}H_{23}IN_2$ (358.26): C, 50.29; H, 6.47; N, 7.82. Found: C, 49.93; H, 6.52; N, 8.03. ^{1}H NMR (300 MHz, $CDCl_3$): δ 1.51 (s, 6H), 1.55–1.70 (m, 6H), 2.00 (s, 3H), 4.00 (s, 2H), 4.14 (s, 3H), 7.30 (s, 1H), 7.62 (s, 1H), 9.90 (s, 1H). ^{13}C{^{1}H} NMR (75 MHz, $CDCl_3$): δ 27.9, 34.1, 36.4, 37.3, 39.8, 61.6, 123.4, 123.9, 137.5. IR (KBr): 3483(m), 3398(m), 3138(w), 3074(m), 2900(s), 2848(s), 2677(w), 2657(w), 1618(w), 1562(m), 1452(m), 1425(w), 1342(w), 1209(w), 1169(s), 1136(w), 1107(w), 833(m), 810(m), 781(w), 752(m), 719(w), 665(m), 621(m) cm^{-1}. ESI-MS: m/z 231.1 [M]$^+$ (100%).

*1-(1-Adamantylmethyl)-3-butylimidazolium Bromide (**2**$^+$**Br**$^-$).* The bromide of **2**$^+$ was isolated as tan highly viscous oil (238 mg, 79% yield) using 186 mg (0.86 mmol) of **8**. Anal. Calcd for $C_{18}H_{29}BrN_2$ (353.34): C, 61.19; H, 8.27; N, 7.93. Found: C, 61.36; H, 8.22; N, 8.21. ^{1}H NMR (300 MHz, $CDCl_3$): δ 0.94 (t, J = 7.2 Hz, 3H), 1.37 (m, 2H), 1.50 (s, 6H), 1.62 (m, 6H), 1.91 (m, 2H), 1.99 (s, 3H), 4.02 (s, 2H), 4.39 (t, J = 7.3 Hz, 2H), 7.27 (s, 1H), 7.52 (s, 1H), 10.26 (s, 1H). ^{13}C{^{1}H} NMR (75 MHz, $CDCl_3$): δ 13.7, 19.7, 28.0, 32.4, 34.2, 36.5, 40.0, 50.2, 61.7, 121.9, 124.1, 137.1. IR (KBr): 3464(s), 3410(s), 3132(w), 3069(w), 2958(w), 2903(s), 2848(m), 2677(w), 2658(w), 1633(w), 1561(m), 1453(m), 1370(w), 1316(w), 1162(s), 1135(w), 1106(w), 773(w), 755(w), 717(w), 665(w) cm^{-1}. ESI-MS: m/z 625.3 [2·M$^+$ + ^{79}Br$^-$]$^+$ (8%), 273.3 [M]$^+$ (100%).

*1-[4-(1-Adamantylcarbonyl)benzyl]-3-methylimidazolium Iodide (**3**$^+$**I**$^-$).* The iodide of **3**$^+$ was isolated as pale yellow crystalline powder (196 mg, 83% yield) using 164 mg (0.51 mmol) of **9**. Mp: 162–167 °C. Anal. Calcd for $C_{22}H_{27}IN_2O$ (462.37): C, 57.15; H, 5.89; N, 6.06. Found: C, 57.02; H, 5.91; N, 6.17. ^{1}H NMR (300 MHz, DMSO-d_6): δ 1.69 (s, 6H), 1.89 (s, 6H), 2.01 (s, 3H), 3.87 (s, 3H), 5.49 (s, 2H), 7.46 (d, J = 7.5 Hz, 2H), 7.58 (d, J = 7.2 Hz, 2H), 7.74 (s, 1H), 7.82 (s, 1H), 9.24 (s, 1H). ^{13}C{^{1}H} NMR (75 MHz, DMSO-d_6): δ 27.4, 35.8, 35.9, 38.3, 46.0, 51.4, 122.4, 124.0, 127.4, 127.8, 136.7, 136.8, 139.2, 208.7. IR (KBr): 3164(m), 3135(m), 3056(s), 2971(w), 2911(s), 2850(s), 2677(w), 2656(w), 1735(w), 1671(s), 1608 (w), 1573(m), 1558(m), 1450(m), 1412(w), 1269(m), 1240(m), 1171(s), 1024(w), 987(m), 967(w), 952(w), 834(m), 754(m), 730(m), 692(w), 670(w), 610(m) cm^{-1}. ESI-MS: m/z 335.3 [M]$^+$ (100%).

*1-[4-(1-Adamantylcarbonyl)benzyl]-3-butylimidazolium Bromide (**4**$^+$**Br**$^-$).* The bromide of **4**$^+$ was isolated as tan viscous oil (129 mg, 43% yield) using 212 mg (0.66 mmol) of **9**. Anal. Calcd for $C_{25}H_{33}BrN_2O$ (457.45): C, 65.64; H, 7.27; N, 6.12. Found: C, 65.82; H, 7.35; N, 5.97. ^{1}H NMR (300 MHz, $CDCl_3$): δ 0.94 (t, J = 7.2 Hz, 3H), 1.35 (m, 2H), 1.72 (m, 6H), 1.87–1.94 (m, 2 + 6H), 2.05 (s, 3H), 4.28 (t, J = 7.2 Hz, 2H), 5.70 (s, 2H), 7.35 (s, 1H), 7.44 (s, 1H), 7.50 (d, J = 8.1 Hz, 2H), 7.59 (d, J = 8.4 Hz, 2H), 10.57 (s, 1H). ^{13}C{^{1}H} NMR (75 MHz, $CDCl_3$): δ 13.6, 19.7, 28.2, 32.2, 36.6, 39.1, 47.2, 50.2, 52.9, 122.2, 128.1, 128.9, 135.3, 137.3, 140.8, 210.0. IR (KBr): 3432(s), 3131(w), 3063(w), 2906(s), 2850(m), 2678(w), 2658(w), 1668(m), 1609(w), 1561(m), 1453(m), 1411(w), 1271(m), 1237(m), 1160(m), 988(w), 930(w), 765(w), 684(w), 617(w) cm^{-1}. ESI-MS: m/z 833.4 [2·M$^+$ + ^{79}Br$^-$]$^+$ (3%), m/z 377.3 [M]$^+$ (100%).

*1-(1-Adamantylmethyl)-3-methylbenzoimidazolium Iodide (**5**$^+$**I**$^-$).* The iodide of **5**$^+$ was isolated as colorless crystalline powder (125 mg, 83% yield) using 98 mg (0.37 mmol) of **10**. Mp: 115–120 °C. Anal. Calcd for $C_{19}H_{25}IN_2$ (408.32): C, 55.89; H, 6.17; N, 6.86. Found: C, 55.55; H, 6.17; N, 7.03. ^{1}H NMR (300 MHz, DMSO-d_6): δ 1.56–1.67 (m, 12H), 1.95 (s, 3H), 4.11 (s, 3H), 4.23 (s, 2H), 7.67–7.70 (m, 2H), 8.01–8.03 (m, 1H), 8.12–8.14 (m, 1H), 9.64 (s, 1H). ^{13}C{^{1}H} NMR (75 MHz, DMSO-d_6): δ 27.4, 33.3, 34.3, 35.9, 39.0, 57.0, 113.4, 114.1, 126.2, 126.4, 131.5, 132.3, 143.2. IR (KBr): 3467(m), 3442(m), 3134(w), 3010(w), 2902(s), 2848(m), 1618(w), 1566(m), 1487(w), 1456(m), 1344(w), 1313(w), 1275(w), 1209(w), 1024(w), 845(w), 762(m), 750(w), 569(w), 428 (w) cm^{-1}. ESI-MS: m/z 281.2 [M]$^+$ (100%).

*1-(1-Adamantylmethyl)-3-butylbenzoimidazolium Bromide (**6**$^+$**Br**$^-$).* The bromide of **6**$^+$ was isolated as colorless crystalline powder (279 mg, 92% yield) using 200 mg (0.75 mmol) of **10**. Mp: 208–212 °C. Anal. Calcd for $C_{22}H_{31}BrN_2$ (403.40): C, 66.50; H, 7.75; N, 6.94. Found: C, 66.27; H, 7.83; N, 7.05. ^{1}H NMR (300 MHz, $CDCl_3$): δ 0.96 (t, J = 7.2 Hz, 3H), 1.43 (m, 2H), 1.54–1.69 (m, 12H), 1.99–2.06 (m, 5H), 4.31 (s, 2H), 4.68 (t, J = 7.5 Hz, 2H), 7.61–7.74 (m, 4H), 11.17 (s, 1H). ^{13}C{^{1}H} NMR (75 MHz, $CDCl_3$): δ 13.7, 19.9, 28.0, 31.5, 35.2, 36.4, 40.4, 47.6, 58.7, 113.1, 114.0, 127.0, 127.2, 131.0, 132.9, 143.6. IR (KBr): 3454(m), 3387(m), 3129(w), 3056(w), 3029(w), 2964(m), 2904(s), 2849(m), 2789(w), 2679(w), 1614(w), 1564(s), 1480(w), 1458(m), 1428(m), 1386(m), 1369(w), 1346(w), 1316(w), 1278(w), 1230(w), 1212(w), 762(s), 616(w) cm^{-1}. ESI-MS: m/z 725.3 [2·M$^+$ + ^{79}Br$^-$]$^+$ (10%), m/z 323.2 [M]$^+$ (100%).

*1-(1-Adamantylmethyl)-3-butylbenzoimidazolium Iodide (**6**$^+$**I**$^-$).* The iodide of **6**$^+$ was isolated as colorless crystalline powder (128 mg, 86% yield) using 89 mg (0.33 mmol) of **10**. Mp: 202–204 °C. Anal. Calcd for $C_{22}H_{31}IN_2$ (450.40): C, 58.67; H, 6.94; N, 6.22. Found: C, 58.43; H, 6.86; N, 6.23. ^{1}H NMR (300 MHz, $CDCl_3$): δ 0.98 (t, J = 7.2 Hz, 3H), 1.46 (m, 2H), 1.55–1.66 (m, 12H), 2.01–2.09 (m, 5H), 4.33 (s, 2H), 4.68 (t, J = 7.5 Hz, 2H), 7.63–7.79 (m, 4H), 10.91 (s, 1H). ^{13}C{^{1}H} NMR (75 MHz, $CDCl_3$): δ 13.7, 19.9, 28.0, 31.5, 35.2, 36.4, 40.5, 47.6, 58.7, 113.2, 114.1, 127.2, 127.4, 131.0, 132.8, 142.6. IR (KBr): 3126(w), 3023(w), 2994(w), 2965(m), 2901(s), 2847(m), 2676(w), 2657(w), 1612(w), 1563(s), 1488(w), 1459(m), 1430(m), 1367(w), 1347(w), 1315(w), 1277(w), 1207(w), 1180(w), 1022(w), 758(s), 615(w), 571(w) cm^{-1}. ESI-MS: m/z 773.3 [2·M$^+$ + I$^-$]$^+$ (21%), m/z 323.3 [M]$^+$ (100%).

*1-(1-Adamantylmethyl)-3-butylbenzoimidazolium Mesylate (**6**$^+$**MsO**$^-$).* The mesylate of **6**$^+$ was isolated as colorless crystalline powder (57 mg, 36% yield) using 100 mg (0.38 mmol) of **10**. Mp: 195–198 °C. Anal. Calcd for $C_{23}H_{34}N_2O_3S$ (418.59): C, 65.99; H, 8.19; N, 6.69. Found: C, 66.17; H, 8.12; N, 6.92. ^{1}H NMR (300 MHz, $CDCl_3$): δ 0.98 (t, J = 7.5 Hz, 3H), 1.45 (m, 2H), 1.56–1.71 (m, 12H), 2.01–2.07 (m, 5H), 2.80 (s, 3H), 4.28 (s, 2H), 4.64 (t, J = 7.2 Hz, 2H), 7.59–7.71 (m, 4H), 10.57 (s, 1H). ^{13}C NMR (75 MHz, $CDCl_3$): δ 13.6, 19.9, 28.1, 31.5, 35.2, 36.5, 39.8, 40.4, 47.5, 58.6, 113.0, 114.0, 126.8, 126.9, 131.2, 133.0, 144.7. IR (KBr): 3121(w), 3103(w), 3027(w), 2960(w), 2906(s), 2849(m), 2677(w), 1638(w), 1614(w), 1561(m), 1484(w), 1459(w), 1429(w), 1385(w), 1344(w), 1318(w), 1279(w), 1207(s), 1145(w), 1044(s), 1021(w), 772(s), 672(w), 617(w), 553(m) cm^{-1}. ESI-MS: m/z 741.4 [2·M$^+$ + MsO$^-$]$^+$ (2%), m/z 323.3 [M]$^+$ (100%).

*1-[4-(1-Adamantylcarbonyl)benzyl]-3-butylbenzoimidazolium Mesylate (**7**$^+$**MsO**$^-$).* The mesylate of **7**$^+$ was isolated as colorless crystalline powder (24 mg, 17% yield) using 100 mg (0.27 mmol) of **11**. Mp: 193–198 °C. Anal. Calcd for $C_{30}H_{38}N_2O_4S$ (522.70): C,

DOI: 10.1021/acs.joc.6b01564
J. Org. Chem. 2016, 81, 9595–9604

68.93; H, 7.33; N, 5.36. Found: C, 69.07; H, 7.39; N, 5.12. ^{1}H NMR (300 MHz, $CDCl_3$): δ 0.98 (t, J = 6.9 Hz, 3H), 1.45 (m, 2H), 1.71 (m, 6H), 1.92−2.03 (m, 11H), 2.82 (s, 3H), 4.57 (t, J = 6.9 Hz, 2H), 5.89 (s, 2H), 7.50−7.70 (m, 8H), 10.98 (s, 1H). ^{13}C{^{1}H} NMR (75 MHz, $CDCl_3$): δ 13.6, 20.0, 28.2, 31.4, 36.6, 39.1, 39.8, 47.1, 47.8, 51.0, 113.2, 114.0, 127.2, 127.4, 128.1, 128.2, 131.5, 131.7, 135.2, 140.5, 144.0, 209.8. IR (KBr): 3125(w), 3059(w), 2931(s), 2907(s), 2852(m), 2680(w), 2659(w), 1690(m), 1611(w), 1561(m), 1481(w), 1454(w), 1431(w), 1380(w), 1346(w), 1273(w), 1208(s), 1194(s), 1116(w), 1059(m), 1045(m), 989(w), 952(w), 932(w), 854(w), 809(w), 761(m), 670(w), 634(w), 611(w), 555(w), 536(w) cm^{-1}. ESI-MS: m/z 949.4 [2·M$^+$ + MsO$^-$]$^+$ (11%), m/z 427.3 [M]$^+$ (100%).

*General Procedure for Preparation of **9** and **11**.* Benzimidazole or imidazole (1 equiv) was dissolved in dry DMF (150 equiv), and *N*-ethyl-*N*-isopropylpropan-2-amine (1.5 equiv) and 1-adamantyl 4-bromomethylphenyl ketone (1.1 equiv) were added at room temperature. The mixture was vigorously stirred under an inert atmosphere at 100 °C for 5 days. The resulting slurry was poured into crushed ice and extracted with CH_2Cl_2. Collected organic portions were washed with water and brine and dried over Na_2SO_4. Solvents were distilled off in vacuum, and residual DMF was removed via azeotropic distillation with $CHCl_3$. Crude material was purified on column [silica gel, 1:1 (v/v) petroleum ether/ethyl acetate].

*1-[4-(1-Adamantylcarbonyl)benzyl]-1H-imidazole (**9**).* Compound **9** was isolated as pale yellow oil in a yield of 328 mg (65%) using 573 mg (1.72 mmol) of starting bromide. Anal. Calcd for $C_{21}H_{24}N_2O$ (320.43): C, 78.71; H, 7.55; N, 8.74. Found: C, 78.83; H, 7.52; N, 8.51. ^{1}H NMR (300 MHz, $CDCl_3$): δ 1.71−1.81 (m, 6H), 2.00 (s, 6H), 2.09 (s, 3H), 5.28 (s, 2H), 7.00 (s, 1H), 7.23−7.28 (overlapped signals, 3H), 7.56 (d, J = 8.4 Hz, 2H), 8.22 (s, 1H). ^{13}C{^{1}H} NMR (75 MHz, $CDCl_3$): δ 28.3, 36.7, 39.2, 47.2, 50.8, 119.6, 127.0, 128.1, 129.4, 137.5, 138.1, 139.8, 209.6. IR (KBr): 3111(w), 2905(s), 2850(s), 2679(w), 2658(w), 1667(s), 1609(m), 1506(m), 1452(m), 1412(w), 1345(w), 1271(s), 1234(s), 1177(m), 1106(w), 1076(m), 1030(w), 988(m), 954(w), 930(w), 834(w), 815(w), 794(w), 733(m), 663(m) cm^{-1}. GC−MS (EI): m/z 320 (5%), 293 (12%), 292 (50%), 136 (11%), 135 (100%), 118 (9%), 107 (14%), 93 (24%), 91 (9%), 90 (13%), 89 (8%), 81 (9%), 79 (27%), 77 (9%), 67 (11%), 55 (7%), 41 (8%).

*1-[4-(1-Adamantylcarbonyl)benzyl]-1H-benzimidazole (**11**).* Compound **11** was isolated as pale yellow crystalline powder in a yield of 218 mg (44%) using 497 mg (1.49 mmol) of starting bromide. Mp: 126−131 °C. Anal. Calcd for $C_{25}H_{26}N_2O$ (370.49): C, 81.05; H, 7.07; N, 7.56. Found: C, 80.94; H, 7.09; N, 7.38. ^{1}H NMR (300 MHz, $CDCl_3$): δ 1.68−1.78 (m, 6H), 1.96−1.97 (m, 6H), 2.06 (s, 3H), 5.42 (s, 2H), 7.20 (d, J = 8.4 Hz, 2H), 7.27−7.32 (overlapped signals, 3H), 7.52 (d, J = 7.2 Hz, 2H), 7.86 (m, 1H), 8.15 (s, 1H). ^{13}C{^{1}H} NMR (300 MHz, $CDCl_3$): δ 28.3, 36.7, 39.2, 47.1, 48.6, 110.1, 120.7, 122.7, 123.5, 126.7, 128.2, 134.0, 137.8, 139.7, 143.3, 144.0, 209.5. IR (KBr): 3436(w), 3118(w), 3100(w), 3057(w), 3037(w), 3025(w), 2930(s), 2900(s), 2850(s), 2675(w), 2658(w), 1943(w), 1906(w), 1793(w), 1718(w), 1670(s), 1617(w), 1561(w), 1494(s), 1460(m), 1446(m), 1411(w), 1373(m), 1349(m), 1316(w), 1274(m), 1240(m), 1205(w), 1179(m), 1111(w), 1050(w), 1020(w), 986(m), 930(m), 887(w), 845(w), 864(w), 845(w), 821(w), 789(w), 756(s), 722(w), 683(w), 640(w), 608(w), 581(w) cm^{-1}. GC−MS (EI): m/z 371 (8%), 370 (28%), 343 (15%), 342 (55%), 225 (6%), 208 (6%), 136 (11%), 135 (100%), 131 (6%), 119 (8%), 107 (13%), 93 (25%), 91 (12%), 90 (16%), 89 (12%), 81 (8%), 79 (26%), 77 (10%), 67 (11%), 55 (8%), 41 (6%).

Computational Details. The nucleus-independent chemical shielding (NICS[28]) was calculated on geometry-optimized structures of β-CD, CB6, and CB7 at the PBE0[34]/6-311G**[35] level of theory using the Gaussian 09.A2[36] software package. PyMOL[37] and VMD[38] were used to visualize the computed data. Molecular dynamics of individual complexes were performed in the AMBER 12 package[39] using GAFF[40] and GLYCAM06[41] force fields. Production simulations at 300 K and 1 bar in an explicit water environment were 1 μs long. See the Supporting Information for further details.

■ ASSOCIATED CONTENT

Supporting Information

The Supporting Information is available free of charge on the ACS Publications website at DOI: 10.1021/acs.joc.6b01564.

^{1}H and ^{13}C NMR spectra of the new compounds **1**−**7**, crystallographic data for **6**$^+$I$^-$ and **6**$^+$MsO$^-$, mass spectra of the free guests and their complexes, ^{1}H NMR and ITC data related to the titration experiments, and computational details (PDF)

Crystallographic data (CIF)

■ AUTHOR INFORMATION

Corresponding Author

*E-mail: rvicha@ft.utb.cz.

Notes

The authors declare no competing financial interest.

■ ACKNOWLEDGMENTS

This work was financially supported by the Internal Funding Agency of Tomas Bata University in Zlín (IGA/FT/2016/001 to P.B., M.R., and R.V.), by the Czech Science Foundation (16-05961S to R.M.), and by the Ministry of Education, Youth and Sports of the Czech Republic under Project CEITEC 2020 (LQ1601 to P.K.). Computational resources were provided by the CESNET LM2015042 and the CERIT Scientific Cloud LM2015085 under the program "Projects of Large Research, Development, and Innovations Infrastructures".

■ REFERENCES

(1) (a) Jiao, D.; Biedermann, F.; Scherman, O. A. *Org. Lett.* **2011**, *13*, 3044−3047. (b) Ko, Y. H.; Kim, E.; Hwang, I.; Kim, K. *Chem. Commun.* **2007**, 1305−1315. (c) Urbach, A. R.; Ramalingam, V. *Isr. J. Chem.* **2011**, *51*, 664−678. (d) Das, D.; Scherman, O. A. *Isr. J. Chem.* **2011**, *51*, 537−550. (e) Jiang, W.; Wang, Q.; Linder, I.; Klautzsch, F.; Schalley, C. A. *Chem. - Eur. J.* **2011**, *17*, 2344−2348. (f) Liu, Y.; Fang, R.; Tan, X.; Wang, Z.; Zhang, X. *Chem. - Eur. J.* **2012**, *18*, 15650−15654.

(2) (a) Ohga, K.; Takashima, Y.; Takahashi, H.; Kawaguchi, Y.; Yamaguchi, H.; Harada, A. *Macromolecules* **2005**, *38*, 5897−5904. (b) Hasegawa, Y.; Miyauchi, M.; Takashima, Y.; Yamaguchi, H.; Harada, A. *Macromolecules* **2005**, *38*, 3724−3730. (c) Wittenberg, J. B.; Zavalij, P. Y.; Isaacs, L. *Angew. Chem., Int. Ed.* **2013**, *52*, 3690−3694. (d) Takashima, Y.; Yuting, Y.; Otsubo, M.; Yamaguchi, H.; Harada, A. *Beilstein J. Org. Chem.* **2012**, *8*, 1594−1600.

(3) (a) Böhm, I.; Isenbügel, K.; Ritter, H.; Branscheid, R.; Kolb, U. *Angew. Chem., Int. Ed.* **2011**, *50*, 7896−7899. (b) Bertrand, B.; Stenzel, M.; Fleury, E.; Bernard, J. *Polym. Chem.* **2012**, *3*, 377−383. (c) Charlot, A.; Auzély-Velty, R. *Macromolecules* **2007**, *40*, 1147−1158.

(4) (a) Harada, A.; Kobayashi, R.; Takashima, Y.; Hashidzume, A.; Yamaguchi, H. *Nat. Chem.* **2011**, *3*, 34−37. (b) Zheng, Y.; Hashidzume, A.; Harada, A. *Macromol. Rapid Commun.* **2013**, *34*, 1062−1066.

(5) (a) Huang, W.-H.; Liu, S.; Zavalij, P. Y.; Isaacs, L. *J. Am. Chem. Soc.* **2006**, *128*, 14744−14745. (b) Nally, R.; Isaacs, L. *Tetrahedron* **2009**, *65*, 7749−7754. (c) Lemaur, V.; Carroy, G.; Poussigue, F.; Chirot, F.; De Winter, J.; Isaacs, L.; Dugourd, P.; Cornil, J.; Gerbaux, P. *ChemPlusChem* **2013**, *78*, 959−969.

(6) (a) Buschmann, H.-J. *Isr. J. Chem.* **2011**, *51*, 533−536. (b) Girek, T. *J. Inclusion Phenom. Macrocyclic Chem.* **2013**, *76*, 237−252. (c) Kim, K. *Chem. Soc. Rev.* **2002**, *31*, 96−107. (d) Sforazzini, G.; Kahnt, A.; Wykes, m.; Sprafke, J. K.; Brovelli, S.; Montarnal, D.; Meinardi, F.; Cacialli, F.; Beljonne, D.; Albinsson, B.; Anderson, L. H. *J. Phys. Chem. C* **2014**, *118*, 4553−4566. (e) Buschmann, H.-J.; Wego, A.; Jansen, K.; Schollmeyer, E.; Döpp, D. *J. Inclusion Phenom. Mol. Recognit. Chem.* **2005**, *53*, 183−189.

DOI: 10.1021/acs.joc.6b01564
J. Org. Chem. 2016, 81, 9595−9604

(7) (a) Rekharsky, M. V.; Yamamura, H.; Kawai, M.; Osaka, I.; Arakawa, R.; Sato, A.; Ko, Y. H.; Selvapalam, N.; Kim, K.; Inoue, Y. *Org. Lett.* **2006**, *8*, 815−817. (b) Leclercq, L.; Noujeim, N.; Sanon, S. H.; Schmitzer, A. R. *J. Phys. Chem. B* **2008**, *112*, 14176−14184.
(8) (a) Wyman, I. W.; Macartney, D. H. *J. Org. Chem.* **2009**, *74*, 8031−8038. (b) Sinha, M. K.; Reany, O.; Yefet, M.; Botoshansky, M.; Keinan, E. *Chem. - Eur. J.* **2012**, *18*, 5589−5605.
(9) Samsam, S.; Leclercq, L.; Schmitzer, A. R. *J. Phys. Chem. B* **2009**, *113*, 9493−9498.
(10) (a) Isaacs, L. *Chem. Commun.* **2009**, 619−629. (b) Masson, E.; Ling, X.; Joseph, R.; Kyeremeh-Mensah, L.; Lu, X. *RSC Adv.* **2012**, *2*, 1213−1247. (c) Huang, W.-H.; Liu, S.; Isaacs, L. Cucurbit[n]urils. In *Modern Supramolecular Chemistry: Strategy for Macrocycle Synthesis*; Diederich, F., Stang, P. J., Tykwinski, R. R., Eds.; Wiley-VCH: Weinheim, Germany, 2008; pp 113. (d) Barrow, S. J.; Kasera, S.; Rowland, M. J.; del Barrio, J.; Scherman, O. A. *Chem. Rev.* **2015**, *115*, 12320−12406.
(11) (a) Harada, A.; Takashima, Y. *Chem. Rev.* **2013**, *13*, 420. (b) Harada, A.; Takashima, Y.; Nakahata, M. *Acc. Chem. Res.* **2014**, *47*, 2128−2140.
(12) Hashimoto, H. CyD applications in food, cosmetic, toiletry, textile and wrapping material fields. In *Cyclodextrins and Their Complexes*; Dodziuk, H., Ed.; Wiley-VCH: Weinheim, Germany, 2006; pp 452.
(13) Rekharsky, M. V.; Inoue, Y. *Chem. Rev.* **1998**, *98*, 1875−1918.
(14) Freeman, W. A.; Mock, W. L.; Shih, N.-Y. *J. Am. Chem. Soc.* **1981**, *103*, 7367−7368.
(15) Kim, J.; Jung, I. S.; Kim, S. Y.; Lee, E.; Kang, J. K.; Sakamoto, S.; Yamaguchi, K.; Kim, K. *J. Am. Chem. Soc.* **2000**, *122*, 540−541.
(16) Behrend, R.; Meyer, E.; Rusche, F. *Liebigs Ann. Chem.* **1905**, *339*, 1−37.
(17) (a) Rekharsky, M. V.; Mori, T.; Yang, C.; Ko, H. K.; Selvapalam, N.; Kim, H.; Sobransingh, D.; Kaifer, A. E.; Liu, S.; Isaacs, L.; Chen, W.; Moghaddam, S.; Gilson, M. K.; Kim, K.; Inoue, Y. *Proc. Natl. Acad. Sci. U. S. A.* **2007**, *104*, 20737−20742. (b) Yi, S.; Li, W.; Nieto, D.; Cuadrado, I.; Kaifer, A. E. *Org. Biomol. Chem.* **2013**, *11*, 287−293.
(18) Moghaddam, S.; Yang, C.; Rekharsky, M.; Ko, Y. H.; Kim, K.; Inoue, Y.; Gilson, M. K. *J. Am. Chem. Soc.* **2011**, *133*, 3570−3581.
(19) Cao, L.; Šekutor, M.; Zavalij, P. Y.; Mlinarić-Majerski, K.; Glaser, R.; Isaacs, L. *Angew. Chem., Int. Ed.* **2014**, *53*, 988−993.
(20) Chakrabarti, S.; Mukhopadhyay, P.; Lin, S.; Isaacs, L. *Org. Lett.* **2007**, *9*, 2349−2352.
(21) Mukhopadhyay, P.; Zavalij, P. Y.; Isaacs, L. *J. Am. Chem. Soc.* **2006**, *128*, 14093−14102.
(22) Tootoonchi, M. H.; Yi, S.; Kaifer, A. E. *J. Am. Chem. Soc.* **2013**, *135*, 10804−10809.
(23) (a) Wei-Li, D.; Bi, J.; Sheng-Lian, L.; Xu-Biao, L.; Xin-Man, T.; Chak-Tong, A. *Catal. Sci. Technol.* **2014**, *4*, 556−562. (b) Ruan, J.; Xiao, J. *Acc. Chem. Res.* **2011**, *44*, 614−626. (c) Headley, A. D.; Ni, B. *Aldrichimica Acta* **2007**, *40*, 107−117. (d) Lee, S. *Chem. Commun.* **2006**, 1049−1063.
(24) Riduan, S. N.; Zhang, Y. *Chem. Soc. Rev.* **2013**, *42*, 9055−9070.
(25) (a) Cavell, K. *Dalton Trans.* **2008**, 6676−6685. (b) Legrand, F.-X.; Ménand, M.; Sollogoub, M.; Tilloy, S.; Monflier, E. *New J. Chem.* **2011**, *35*, 2061−2065.
(26) (a) Rouchal, M.; Matelová, A.; de Carvalho, F. P.; Bernat, R.; Grbić, D.; Kuřitka, I.; Babinský, M.; Marek, R.; Čmelík, R.; Vícha, R. *Supramol. Chem.* **2013**, *25*, 349−361. (b) Vícha, R.; Rouchal, M.; Kozubková, Z.; Kuřitka, I.; Marek, R.; Branná, P.; Čmelík, R. *Supramol. Chem.* **2011**, *23*, 663−677.
(27) (a) Kolman, V.; Marek, R.; Střelcová, Z.; Kulhánek, P.; Nečas, M.; Švec, J.; Šindelář, V. *Chem. - Eur. J.* **2009**, *15*, 6926−6931. (b) Zhao, N.; Liu, L.; Biedermann, F.; Scherman, O. A. *Chem. - Asian J.* **2010**, *5*, 530−537. (c) Liu, L.; Zhao, N.; Scherman, O. A. *Chem. Commun.* **2008**, 1070−1072. (d) Liu, L.; Nouvel, N.; Scherman, O. A. *Chem. Commun.* **2009**, 3243−3245.
(28) (a) Schleyer, P. v. R.; Maerker, C.; Dransfeld, A.; Jiao, H.; Hommes, N. J. R. v. E. *J. Am. Chem. Soc.* **1996**, *118*, 6317−6318. (b) Babinský, M.; Bouzková, K.; Pipíška, M.; Novosadová, L.; Marek, R. *J. Phys. Chem. A* **2013**, *117*, 497−503. (c) Bouzková, K.; Babinský, M.; Novosadová, L.; Marek, R. *J. Chem. Theory Comput.* **2013**, *9*, 2629−2638.
(29) Wintgens, V.; Biczók, L.; Miskolczy, Z. *Supramol. Chem.* **2010**, *22*, 612−618.
(30) Liu, S.; Ruspic, C.; Mukhopadhyay, P.; Chakrabarti, S.; Zavalij, P. Y.; Isaacs, L. *J. Am. Chem. Soc.* **2005**, *127*, 15959−15967.
(31) Černochová, J.; Branná, P.; Rouchal, M.; Kulhánek, P.; Kuřitka, I.; Vícha, R. *Chem. - Eur. J.* **2012**, *18*, 13633−13637.
(32) Branná, P.; Rouchal, M.; Prucková, Z.; Dastychová, L.; Lenobel, R.; Pospíšil, T.; Maláč, K.; Vícha, R. *Chem. - Eur. J.* **2015**, *21*, 11712−11718.
(33) Ding, Z.-J.; Zhang, H.-Y.; Wang, L.-H.; Ding, F.; Liu, Y. *Org. Lett.* **2011**, *13*, 856−859.
(34) (a) Perdew, J. P.; Ernzerhof, M.; Burke, K. *J. Chem. Phys.* **1996**, *105*, 9982−9985. (b) Adamo, C.; Barone, V. *J. Chem. Phys.* **1999**, *110*, 6158−6170.
(35) Krishnan, R.; Binkley, J. S.; Seeger, R.; Pople, J. A. *J. Chem. Phys.* **1980**, *72*, 650−654.
(36) Frisch, M. J.; Trucks, G. W.; Schlegel, H. B.; Scuseria, G. E.; Robb, M. A.; Cheeseman, J. R.; Scalmani, G.; Barone, V.; Mennucci, B.; Petersson, G. A.; Nakatsuji, H.; Caricato, M.; Li, X.; Hratchian, H. P.; Izmaylov, A. F.; Bloino, J.; Zheng, G.; Sonnenberg, J. L.; Hada, M.; Ehara, M.; Toyota, K.; Fukuda, R.; Hasegawa, J.; Ishida, M.; Nakajima, T.; Honda, Y.; Kitao, O.; Nakai, H.; Vreven, T.; Montgomery, J. A., Jr.; Peralta, J. E.; Ogliaro, F.; Bearpark, M.; Heyd, J. J.; Brothers, E.; Kudin, K. N.; Staroverov, V. N.; Kobayashi, R.; Normand, J.; Raghavachari, K.; Rendell, A.; Burant, J. C.; Iyengar, S. S.; Tomasi, J.; Cossi, M.; Rega, N.; Millam, J. M.; Klene, M.; Knox, J. E.; Cross, J. B.; Bakken, V.; Adamo, C.; Jaramillo, J.; Gomperts, R.; Stratmann, R. E.; Yazyev, O.; Austin, A. J.; Cammi, R.; Pomelli, C.; Ochterski, J. W.; Martin, R. L.; Morokuma, K.; Zakrzewski, V. G.; Voth, G. A.; Salvador, P.; Dannenberg, J. J.; Dapprich, S.; Daniels, A. D.; Farkas, Ö.; Foresman, J. B.; Ortiz, J. V.; Cioslowski, J.; Fox, D. J. *Gaussian 09*, revision A.2; Gaussian Inc.: Wallingford, CT, 2009.
(37) *The PyMOL Molecular Graphics System*, version 1.6.0; Schrödinger, LLC, 2013.
(38) Humphrey, W.; Dalke, A.; Schulten, K. *J. Mol. Graphics* **1996**, *14*, 33−38.
(39) Case, D.; Darden, T.; Cheatham, T.; Simmerling, C.; Wang, J.; Duke, R.; Luo, R.; Walker, R.; Zhang, W.; Merz, K.; Roberts, B.; Hayik, S.; Roitberg, A.; Seabra, G.; Swails, J.; Goetz, A.; Kolossváry, I.; Wong, K.; Paesani, F.; Vanicek, J.; Wolf, R.; Liu, J.; Wu, X.; Brozell, S.; Steinbrecher, T.; Gohlke, H.; Cai, Q.; Ye, X.; Wang, J.; Hsieh, M.; Cui, G.; Roe, D.; Mathews, D.; Seetin, M.; Salomon-Ferrer, R.; Sagui, C.; Babin, V.; Luchko, T.; Gusarov, S.; Kovalenko, A.; Kollman, P. *AMBER 12*; University of California: San Francisco, 2012.
(40) Wang, J. M.; Wolf, R. M.; Caldwell, J. W.; Kollman, P. A.; Case, D. A. *J. Comput. Chem.* **2004**, *25*, 1157−1174.
(41) Kirschner, K. N.; Yongye, A. B.; Tschampel, S. M.; González-Outeiriño, J.; Daniels, C. R.; Foley, B. L.; Woods, R. J. *J. Comput. Chem.* **2008**, *29*, 622−655.

DOI: 10.1021/acs.joc.6b01564
J. Org. Chem. 2016, 81, 9595−9604